GEOLOGIC MAPPING OF THE NW RIM OF HELLAS BASIN, MARS: EVIDENCE FOR AN ANCIENT BURIED LANDSCAPE, David A. Crown[1], Leslie F. Bleamaster III[1], Scott C. Mest[1], John F. Mustard[2], and Mathieu Vincendon[2], [1]Planetary Science Institute, 1700 E. Ft. Lowell Rd., Suite 106, Tucson, AZ 85719; crown@psi.edu, [2]Dept. of Geological Sciences, Brown University, Providence, RI 02912.

Introduction: Hellas basin is the largest (2000+ km across) well-preserved impact structure on Mars and its deepest depositional sink. The Hellas region exhibits a diverse suite of potential water- and ice-related landforms [e.g., 1-2], and thus provides important constraints for evaluating Mars' hydrogeologic and climate histories. The Hellas rim and adjacent highlands are of special interest given the possibility of paleolakes on the basin floor [2-4], recent studies of potential localized fluvial/lacustrine systems [2, 5-17], and evidence for phyllosilicates around and within impact craters north of the basin [18-26].

Geologic Mapping of NW Hellas: We are producing a 1:1.5M-scale geologic map of eight MTM quadrangles (-25312, -25307, -25302, -25297, -30312, -30307, -30302, -30297) along Hellas' NW rim. The map region (22.5-32.5°S, 45-65°E) includes a transect across the cratered highlands of Terra Sabaea, the degraded NW rim of Hellas, and basin interior deposits of NW Hellas Planitia. No previous mapping studies have focused on this region, although it has been included in earlier global and regional maps [27-29].

Research to-date [30-33] has included general terrain characterization, evaluation of geomorphology and stratigraphic relationships, preliminary exploration of compositional signatures using CRISM, and investigation of impact crater distribution, morphometry, and interior deposits, as well as production of geologic maps of two subregions of the larger map area. Geologic mapping of the NW Hellas rim is providing new constraints on the magnitudes, extents, and history of volatile-driven processes as well as a geologic context for mineralogic identifications.

Mapping Results: NE Subregion. Geologic mapping of the NE subregion (22.5-29°S, 57.6-65°E) characterizes the Terra Sabaea plains zone, interpreted to be a depositional shelf formed subsequent to degradation of rugged highland terrain adjacent to the basin rim [30-33]. Terra Sabaea plains are found at elevations intermediate (-1800m – 500m) to those of the highlands of Terra Sabaea proper and the steeper basin rim zone. Eastern Hellas exhibits evidence for widespread deposition at similar elevations, potentially associated with flooding from Reull Vallis, large paleolakes within Hellas, and/or accumulation of atmospheric volatiles due to circulation patterns off of the south pole [e.g., 2, 4, 34-35].

Surface materials in the NE subregion can be divided into the following types: highlands, smooth plains, crater materials, and crater floor deposits. Subunits within both the highlands and plains may be defined as mapping continues; the plains in particular display significant brightness variations in THEMIS IR images. Small valleys dissect plains surfaces and are concentrated on sloping plains deposits at the margins of highland outcrops. Detailed mapping of this sub-region has resulted in identification of more irregular depressions than were found initially [30] (Figure 1). In some cases, the scarps defining these depressions reveal finely layered outcrops. The occurrence of the irregular depressions and layered outcrops in both crater floor deposits and within the plains may indicate emplacement of sedimentary units on a regional scale. Mapping shows an eroded and extensively buried ancient highland landscape (Figure 2), with partial exhumation indicated by etched surfaces and retreat of plains around eroded massifs and crater rims [32-33].

Mapping Results: NW Subregion. Geologic mapping of the NW subregion (22.5°-30°S, 45-50°E) characterizes the highlands of Terra Sabaea, which typically are found at elevations above 500m and exhibit numerous impact craters with various sizes and degradation states. Irregular depressions exposing layered deposits have been identified in crater interiors [30-33]. This region is located at higher elevations and contains generally larger impact craters with extensive ejecta deposits relative to the NE subregion, and, in general, resembles a typical highland terrain. However, closer inspection during detailed mapping reveals that the units defined for the NE subregion characterize the surface geology of the NW subregion as well. MRO Context Camera (CTX; ~5 m/pixel) images show evidence for burial and partial exhumation of what appear to be relatively well-preserved crater rim and ejecta materials (e.g., 24.9°S, 46.1°E) in lower resolution images. CTX images also show that variations in brightness of plains materials seen in THEMIS IR images can be attributed to differential removal of layered sequences. These geologic characteristics are consistent with burial of ancient cratered terrain extending to the higher elevations of Terra Sabaea.

Correlation of CRISM Mineralogy to Geologic Mapping. We are analyzing CRISM multispectral data for the NW Hellas map area for phyllosilicates and Fe-bearing silicates (olivine-pyroxene). Initial work has focused on the distribution of 67 exposures of smectite identified in the map area with respect to their geologic

setting. Fe/Mg smectites are identified in CRISM data on the basis of vibrational absorptions near 2.3 µm. Individual exposures typically consist of 10s to 100s of pixels grouped together in a localized area. Slightly less than 2/3 are associated with local topographic highs and slightly less than 1/3 with local lows, including irregular depressions in layered materials. Most smectite exposures are found in the highlands or associated with crater rims, but they also occur within the plains and on crater floors. Systematic analysis of the relationships between mineral signatures, geologic setting, and age will help to constrain the geologic evolution of NW Hellas and its climate history. A particular focus will be to understand if phyllosilicates are confined to deposits predating the widespread smooth plains or have a more complicated stratigraphic distribution.

Conclusions: Geologic mapping and investigations of impact craters on the NW Hellas rim [30-33] a) show the presence of Noachian crater populations, b) provide both observational and morphometric evidence for crater infilling and regional resurfacing, and c) reveal an extensively buried landscape, with exhumation around remnants of highland terrain and within crater interiors, exposing layered deposits. Our studies to-date suggest that regional sedimentary deposition extended beyond the topographic margin of Hellas basin and well into the surrounding highlands.

References: [1] Tanaka, K.L. and G.J. Leonard (1995), JGR, 100, 5407-5432. [2] Crown, D.A. et al. (2005), JGR, 110, E12S22, doi:10.1029/2005JE002496. [3] Moore, J.M. and D.E. Wilhelms (2001), Icarus, 154, 258-276. [4] Bleamaster, L.F. and D.A. Crown (2009), in USGS edit. [5] Lahtela, H. et al. (2003), Vernadsky Institute-Brown University Microsymposium 38, MS057. [6] Lahtela, H. et al. (2005), LPSC XXXVI, abstract 1683, LPI (CD-ROM). [7] Ansan, V. and N. Mangold (2004), 2nd Conf. on Early Mars, abstract 8006, LPI (CD-ROM). [8] Ivanov, M.A. et al. (2005), JGR, 110, E12S21, doi:10.1029/2005JE002420. [9] Korteniemi, J. et al. (2005), JGR, 110, E12S18, doi:10.1029/2005JE002427. [10] Kraal, E.R. et al. (2005), Role of Volatiles on Martian Impact Craters, abstract 3008, LPI (CD-ROM). [11] Mest, S.C. and D.A. Crown (2005), Icarus, 175(2), 335-359. [12] Mest, S.C. (2005), Role of Volatiles on Martian Impact Craters, abstract 3014, LPI (CD-ROM). [13] Mest, S.C. (2006), LPSC XXXVII, abstract 2236, LPI (CD-ROM). [14] Moore, J.M. and A.D. Howard (2005), JGR, 110, E04005, doi:10.1029/2004JE002352. [15] Moore, J.M. and A.D. Howard (2005), LPSC XXXVI, abstract 1512, LPI (CD-ROM). [16] Wilson, S.A. and A.D. Howard (2005), LPSC XXXVI, abstract 2060, LPI (CD-ROM). [17] Wilson, S.A. et al. (2007), JGR, 112, E08009, doi:10.1029/2006JE002830. [18] Poulet, F. et al. (2005), Nature, 438, 623-627. [19] Bibring, J.-P. et al. (2006), Science, 312, 400-404. [20] Costard, F. et al. (2006), LPSC XXXVII, abstract 1288, LPI (CD-ROM). [21] Murchie, S. et al. (2006), EOS Trans. AGU, abstract P33A-04. [22] Murchie, S. et al. (2007), JGR, 112, E05S03, doi:10.1029/2006JE002682. [23] Mustard, J.F. et al. (2007), LPSC XXXVIII, abstract 2071, LPI (CD-ROM). [24] Mustard, J.F. et al. (2007), 7th Inter. Conf. on Mars, LPI. [25] Pelkey, S.M. et al. (2007), LPSC XXXVIII, abstract 1994, LPI (CD-ROM). [26] Pelkey, S.M. et al. (2007), JGR, 112, E08S14, doi:10.1029/2006JE002831. [27] Scott, D.H. and M.H. Carr (1978), USGS Misc. Invest. Ser. Map, I-1083. [28] Greeley, R. and J.E. Guest (1987), USGS Misc. Invest. Ser. Map I-1802B. [29] Leonard, G.J. and K.L. Tanaka (2001), USGS Geol. Invest. Ser. Map I-2694. [30] Crown, D.A. et al. (2007), EOS Trans. AGU, abstract P41A-0189. [31] Mest, S.C. et al. (2008), LPSC XXXIX, abstract 1704, LPI (CD-ROM). [32] Crown, D.A. et al. (2009), LPSC XL, abstract 1705, LPI (CD-ROM). [33] Crown, D.A. et al. (2009), NASA-CP, in press. [34] Colaprete, A. et al. (2004), LPSC XXXV, abstract 2149, LPI (CD-ROM). [35] Colaprete, A. et al. (2005), Nature, 435, 184-188.

Figure 1. CTX image (P12_005803_1532; centered at 61.76°E, 26.45°S; scene width = 17.5 km) showing irregular depression revealing layered deposits.

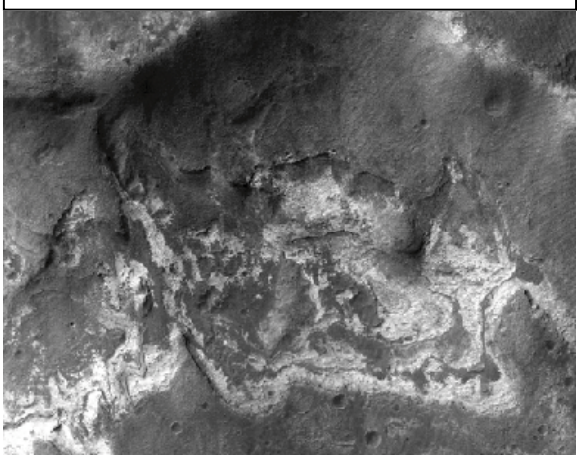

Figure 2. THEMIS IR mosaic (centered at 60.15°E, 24.14°S) showing buried landscape, etched surfaces of plains, scarps, and valleys. Buried crater (right of center) is 17 km across.